A Multigrid Method for Coupled Optimal Topology and Shape Design in Nonlinear Magnetostatics *

Dalibor Lukáš

Department of Applied Mathematics, VŠB–Technical University of Ostrava
dalibor.lukas@vsb.cz

Summary. Topology optimization searches for an optimal distribution of material and void without any restrictions on the structure of the design geometry. Shape optimization tunes the shape of the geometry, while the topology is fixed. In the paper we propose a sequential coupling so that a coarsely optimized topology is the initial guess for the following shape optimization. We aim at making this algorithm fast by using the adjoint sensitivity analysis to the Newton-method for the governing nonlinear state equation and a multigrid approach for the shape optimization. A finite element discretization method is employed. Numerical results are given for a 2–dimensional optimal design of a direct electric current electromagnet.

1 Introduction

In the process of development of industrial components one looks for the parameters to be optimal subject to a proper criterion. The geometry is usually crucial as far as the design of electromagnetic components is concerned. We can employ topology optimization, cf. [Ben95], to find an optimal distribution of the material without any preliminary knowledge. Shape optimization, cf. [HN97, Luk04], is used to tune shapes of a known initial design. While in the structural mechanics topology optimization results in rather complicated structures the shapes of which are not needed to be then optimized, in magnetostatics we end up with simple topologies which, however, serve as very good initial guesses for the further shape optimization. The idea here is to couple them sequentially.

In [Cea00] a connection between topological and shape gradient is shown and applied in structural mechanics. They proceed shape and topology optimization simultaneously so that at one optimization step both the shape and

* This research has been supported by the Czech Ministry of Education under the grant AVČR 1ET400300415 and by the Czech Grant Agency under the grant GAČR 201/05/P008.

topology gradient are calculated. Then shapes are displaced and the elements with great values of the topology gradient are removed, while introducing the natural boundary condition along the new parts, e.g. a hole. Here we are rather motivated by the approach in [OBR91, TCh01]. In the latter they apply a similar algorithm as we do to structural mechanics, however, using re-meshing in a CAD software environment, which was computationally very expensive. Our aim here is to make the algorithm fast. Therefore, we additionally employ semianalytical sensitivity analysis and a multilevel method.

2 Topology optimization for magnetostatics

Let $\Omega \subset \mathbf{R}^2$ be a convex computational domain that is divided into a Lipschitz subdomain $\Omega_{\rm d} \subset \Omega$, where the optimal distribution of the ferromagnetics and the air is to be find, and into the air Lipschitz subdomain $\Omega_0 := \Omega \setminus \overline{\Omega_{\rm d}}$. Let further $Q := \{\rho \in L^2(\Omega_{\rm d}) : 0 \le \rho \le 1,\ \int_{\Omega_{\rm d}} \widetilde{\rho}(\rho)\, d\mathbf{x} \le V_{\max}\}$ be a set of admissible material distributions, where $V_{\max} > 0$ is a maximal possible area occupied by the ferromagnetics and where $\widetilde{\rho} \in C^2((0,1))$ penalizes the values of $\rho \in [0, 1/2)$ to vanish and the values of $\rho \in (1/2, 1]$ to approach 1 as follows:

$$\widetilde{\rho}(\rho) \equiv \widetilde{\rho}_{p_\rho}(\rho) := \frac{1}{2}\left(1 + \frac{1}{\arctan(p_\rho)}\arctan(p_\rho(2\rho - 1))\right).$$

Finally, let $J : H^1(\Omega) \mapsto \mathbf{R}$ be a cost functional. We consider the following topology optimization problem:

$$\text{Find } \rho^* \in Q : J(u(\rho^*)) \le J(u(\rho)) \quad \forall \rho \in Q \tag{1}$$

with respect to the 2-dimensional nonlinear magnetostatic state problem: Find $u(\rho) \in H^1_0(\Omega)$ so that

$$\begin{aligned} \forall v \in H^1_0(\Omega) : \quad & \int_\Omega \nu_0\, \mathbf{grad}(u(\rho)) \cdot \mathbf{grad}(v)\, d\mathbf{x} \\ + \int_{\Omega_{\rm d}} \widetilde{\rho}(\rho)\, \nu(\|\mathbf{grad}(u(\rho))\|)\, \mathbf{grad}(u(\rho)) \cdot \mathbf{grad}(v)\, d\mathbf{x} &= \int_\Omega J v\, d\mathbf{x}, \end{aligned} \tag{2}$$

where $\nu \in C^2((0,\infty))$ denotes a nonlinear material reluctivity of the ferromagnetics, $\nu_0 := 4\pi 10^{-7}$ [H/m] is the vacuum reluctivity constant and $J \in L^2(\Omega)$ is a current density. Note that in general, one has to pose an additional regularization of the topology ρ to avoid the so-called checkerboard effect. However, we are merely interested in a coarsely discretized problem, for which this ill-posedeness is neglectable.

2.1 Nonlinear State Sensitivity Analysis

When solving the problem (1), we use a nested approach, i.e. for a given design we eliminate the nonlinear state equation (2). The latter is discretized by the

finite element method using the linear Lagrange nodal elements on triangles, which reads as follows:

$$\mathbf{A}(\mathbf{u}(\boldsymbol{\rho}), \boldsymbol{\rho}) \cdot \mathbf{u}(\boldsymbol{\rho}) = \mathbf{f}, \tag{3}$$

where $\mathbf{A} \in \mathbb{R}^{n \times n}$ is the assembled reluctivity matrix, $\mathbf{f} \in \mathbb{R}^n$ is the right-hand side vector, $\mathbf{u} \in \mathbb{R}^n$ is the solution vector and $\boldsymbol{\rho} \in \mathbb{R}^m$ is the element-wise constant material function.

The problem (3) is solved by the Newton method. Moreover, the optimization algorithm under consideration requires the gradients of the cost functional with respect to $\boldsymbol{\rho}$. To this goal, we derived the corresponding adjoint Newton method by differentiating the original Newton method in the backward sense. The algorithms are depicted below. Note that for both of them the amount of computational work is the same.

Newton method

Given $\boldsymbol{\rho}$
$i := 0$
Solve $\mathbf{A}(\mathbf{0}, \boldsymbol{\rho}) \cdot \mathbf{u}^0 = \mathbf{f}$
$\mathbf{f}^0 := \mathbf{f} - \mathbf{A}(\mathbf{u}^0, \boldsymbol{\rho}) \cdot \mathbf{u}^0$
while $\|\mathbf{f}^i\| / \|\mathbf{f}\| >$ prec **do**
  $i := i + 1$
  Solve $\mathbf{A}'_{\mathbf{u}}(\mathbf{u}^{i-1}, \boldsymbol{\rho}) \cdot \mathbf{w}^i = \mathbf{f}^{i-1}$
  Find $\tau^i : \|\mathbf{f}^i(\tau^i)\| < \|\mathbf{f}^{i-1}\|$
  $\mathbf{u}^i := \mathbf{u}^{i-1} + \tau^i \mathbf{w}^i$
  $\mathbf{f}^i := \mathbf{f} - \mathbf{A}(\mathbf{u}^i, \boldsymbol{\rho}) \cdot \mathbf{u}^i$
  Store $\mathbf{w}^i$ and τ^i
end while
Store $\mathbf{u}^i$ and $k := i$
Calculate objective $J(\mathbf{u}^i, \boldsymbol{\rho})$

Adjoint Newton method

Given $\boldsymbol{\rho}$, k, $\mathbf{u}^k$, $\{\mathbf{w}^i\}_{i=1}^k$ and $\{\tau^i\}_{i=1}^k$
$\boldsymbol{\lambda} := J'_{\mathbf{u}}(\mathbf{u}^k, \boldsymbol{\rho})$
$\omega := \mathbf{0}$
for $i := k, \ldots, 1$ **do**
  $\mathbf{u}^{i-1} := \mathbf{u}^i - \tau^i \mathbf{w}^i$
  Solve $\mathbf{A}'_{\mathbf{u}}(\mathbf{u}^{i-1}, \boldsymbol{\rho})^T \cdot \boldsymbol{\eta} = \boldsymbol{\lambda}$
  $\boldsymbol{\omega} := \boldsymbol{\omega} + \tau^i \mathbf{G}_{\boldsymbol{\rho}}(\mathbf{u}^{i-1}, \mathbf{w}^i, \boldsymbol{\rho})^T \cdot \boldsymbol{\eta}$
  $\boldsymbol{\lambda} := \boldsymbol{\lambda} + \tau^i \mathbf{G}_{\mathbf{u}}(\mathbf{u}^{i-1}, \mathbf{w}^i, \boldsymbol{\rho})^T \cdot \boldsymbol{\eta}$
end for
Solve $\mathbf{A}(\mathbf{0}, \boldsymbol{\rho})^T \cdot \boldsymbol{\eta} = \boldsymbol{\lambda}$
$\frac{dJ(\mathbf{u}^k(\boldsymbol{\rho}), \boldsymbol{\rho})}{d\boldsymbol{\rho}} := \boldsymbol{\omega} + \mathbf{H}_{\boldsymbol{\rho}}(\mathbf{u}^0, \boldsymbol{\rho})^T \cdot \boldsymbol{\eta} + J'_{\boldsymbol{\rho}}(\mathbf{u}^k, \boldsymbol{\rho})$

The sensitivity information of the system matrix is involved in the following matrices:

$$\begin{aligned}
\mathbf{G}_{\boldsymbol{\rho}}(\mathbf{u}, \mathbf{w}, \boldsymbol{\rho}) &:= -\left[\frac{\partial \mathbf{A}'_{\mathbf{u}}(\mathbf{u}, \boldsymbol{\rho})}{\partial \rho_1} \cdot \mathbf{w}, \ldots, \frac{\partial \mathbf{A}'_{\mathbf{u}}(\mathbf{u}, \boldsymbol{\rho})}{\partial \rho_m} \cdot \mathbf{w}\right] \\
&\quad - \left[\frac{\partial \mathbf{A}(\mathbf{u}, \boldsymbol{\rho})}{\partial \rho_1} \cdot \mathbf{u}, \ldots, \frac{\partial \mathbf{A}(\mathbf{u}, \boldsymbol{\rho})}{\partial \rho_m} \cdot \mathbf{u}\right], \\
\mathbf{G}_{\mathbf{u}}(\mathbf{u}, \mathbf{w}, \boldsymbol{\rho}) &:= -\left[\frac{\partial \mathbf{A}'_{\mathbf{u}}(\mathbf{u}, \boldsymbol{\rho})}{\partial u_1} \cdot \mathbf{w}, \ldots, \frac{\partial \mathbf{A}'_{\mathbf{u}}(\mathbf{u}, \boldsymbol{\rho})}{\partial u_n} \cdot \mathbf{w}\right] - \mathbf{A}'_{\mathbf{u}}(\mathbf{u}, \boldsymbol{\rho}), \\
\mathbf{H}_{\boldsymbol{\rho}}(\mathbf{u}, \boldsymbol{\rho}) &:= -\left[\frac{\partial \mathbf{A}(\mathbf{0}, \boldsymbol{\rho})}{\partial \rho_1} \cdot \mathbf{u}, \ldots, \frac{\partial \mathbf{A}(\mathbf{0}, \boldsymbol{\rho})}{\partial \rho_m} \cdot \mathbf{u}\right],
\end{aligned}$$

where $\mathbf{A}'_{\mathbf{u}}(\mathbf{u}, \boldsymbol{\rho})$ is the linearization of the nonlinear system matrix. We only need to implement their applications, which can be efficiently performed element-wise.

3 Sequential Coupling of Topology and Shape Optimization

We will use the optimal topology design as the initial guess for the shape optimization. The first step towards a fully automatic procedure is a shape identification, which we are doing by hand for the moment. For this purpose, one can use a binary image components recongnition based on boundary tracing, which is a well-known algorithm in the image processing, cf. [GW92]. The second step we are treating here is a piecewise smooth approximation of the boundaries by Bézier curves. Let $\rho^{\rm opt} \in \mathcal{Q}$ be an optimized discretized material distribution. Recall that it is not a strictly 0-1 function. Let $\mathbf{p}_1 \in \mathbb{R}^{m_1}, \ldots, \mathbf{p}_s \in \mathbb{R}^{m_s}$ denote vectors of Bézier parameters of the shapes $\alpha_1(\mathbf{p}_1), \ldots, \alpha_s(\mathbf{p}_s)$ which form the interface between the air and ferromagnetic subdomains $\Omega_0(\alpha_1, \ldots, \alpha_s)$ and $\Omega_1(\alpha_1, \ldots, \alpha_s)$, respectively, i.e. $\Omega_1 \subset \Omega_{\rm d}$, $\overline{\Omega} = \overline{\Omega_0} \cup \overline{\Omega_1}$ and $\Omega_0 \cap \Omega_1 = \emptyset$. Let further $\underline{\mathbf{p}_i}$ and $\overline{\mathbf{p}_i}$ denote the lower and upper bounds, respectively, and let $\mathcal{P} := \left\{(\mathbf{p}_1, \ldots, \mathbf{p}_s) \mid \underline{\mathbf{p}_i} \le \mathbf{p}_i \le \overline{\mathbf{p}_i} \text{ for } i = 1, \ldots, s\right\}$ be the set of admissible Bézier parameters. We solve the following least square fitting problem:

$$\min_{(\mathbf{p}_1,\ldots,\mathbf{p}_s)\in\mathcal{P}} \int_{\Omega_{\rm d}} \left(\rho^{\rm opt} - \chi(\Omega_1\left(\alpha_1(\mathbf{p}_1), \ldots, \alpha_s(\mathbf{p}_s)\right))\right)^2 \, d\mathbf{x}, \tag{4}$$

where $\chi(\Omega_1)$ is the characteristic function of Ω_1.

When solving (4) numerically, one encounters the problem of intersection of the Bézier shapes with the mesh on which $\rho^{\rm opt}$ is elementwise constant. In order to avoid it we use the property that the Bézier control polygon converges linearly to the curve, see Fig. 1, under the following refinement procedure:

$$\begin{aligned}
\left[\mathbf{p}_i^{\rm new}\right]_1 &:= \left[\mathbf{p}_i^{\rm old}\right]_1 \\
\left[\mathbf{p}_i^{\rm new}\right]_j &:= \tfrac{j-1}{m_i+1}\left[\mathbf{p}_i^{\rm old}\right]_{j-1} + \tfrac{m_i-j}{m_i+1}\left[\mathbf{p}_i^{\rm old}\right]_j, \; j = 2, \ldots, m_i, \\
\left[\mathbf{p}_i^{\rm new}\right]_{m_i+1} &:= \left[\mathbf{p}_i^{\rm old}\right]_{m_i}.
\end{aligned}$$

This procedure adds one control node so that the resulting Bézier curve remains unchanged. After a sufficient number of such refinements, the integration in (4) is replaced by a sum over the elements and we deal with intersecting the mesh with a polygon. Note that our least square functional is not twice differentiable whenever a shape touches the grid. This is still acceptable for the quasi-Newton optimization method that we apply.

4 Multilevel Shape Optimization

With the previous notation, the shape optimization problem under consideration is as follows:

$$\begin{aligned}
&\text{Find } (\mathbf{p}_1^*, \ldots, \mathbf{p}_s^*) \in \mathcal{P}: \quad \forall (\mathbf{p}_1, \ldots, \mathbf{p}_s) \in \mathcal{P}: \\
&J(u(\mathbf{p}_1^*, \ldots, \mathbf{p}_s^*)) \le J(u(\mathbf{p}_1, \ldots, \mathbf{p}_s))
\end{aligned} \tag{5}$$

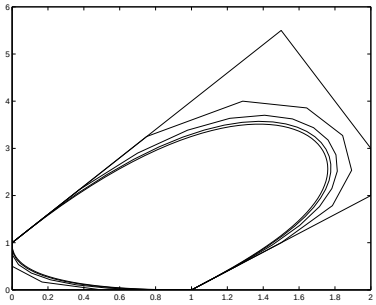

Fig. 1. Approximation of Bézier shapes by the refined control polygon

subject to the 2-dimensional nonlinear magnetostatics: Find $u(\mathbf{p}_1, \ldots, \mathbf{p}_s) \in H_0^1(\Omega)$:

$$\begin{aligned}
\forall v \in H_0^1(\Omega): \quad & \int\limits_{\Omega_0(\alpha_1(\mathbf{p}_1),\ldots,\alpha_s(\mathbf{p}_s))} \nu_0\, \mathbf{grad}(u(\mathbf{p}_1, \ldots, \mathbf{p}_s)) \cdot \mathbf{grad}(v)\, d\mathbf{x} \\
+ & \int\limits_{\Omega_1(\alpha_1(\mathbf{p}_1),\ldots,\alpha_s(\mathbf{p}_s))} \nu(\|\mathbf{grad}(u(\mathbf{p}_1, \ldots, \mathbf{p}_s))\|)\, \mathbf{grad}(u(\mathbf{p}_1, \ldots, \mathbf{p}_s)) \cdot \mathbf{grad}(v)\, d\mathbf{x} \\
= & \int_\Omega Jv\, d\mathbf{x}.
\end{aligned} \tag{6}$$

Concerning the finite element discretization, throughout the optimization we use the following moving grid approach: The control design nodes interpolate the Bézier shape and the remaining grid nodes displacements are given by solving an auxiliary discretized linear elasticity problem with the zero load and the nonzero Dirichlet boundary condition along the design shape that corresponds to the shape displacement. Then, we develop a fairly similar adjoint algorithm for the shape sensitivity analysis as in case of topology optimization.

Perhaps, the main reason for solving the coarse topology optimization as a preprocessing is that we get rid of a large number of design variables in case of fine discretized topology optimization. Once we have a good initial shape design, we will proceed the shape optimization in a multilevel way in order to speed up the algorithm as much as possible. We propose to couple the outer quasi-Newton method with the nested Newton method for eliminitaion of the nonlinear state problem, see the algorithm below. At each iteration of the nested Newton method we employ the conjugate gradient method preconditioned by a geometric multigrid (PCG) so that only one preconditioner per level is used for both the system matrix $\mathbf{A}^{(l)}$ as well as for the linearization $\mathbf{A}^{(l)}{}'_{\mathbf{u}}$, where $\mathbf{A}^{(l)} := \mathbf{A}^{(l)}(\mathbf{p}_1, \ldots, \mathbf{p}_s)$ denotes the reluctivity matrix assembled at the l-th level.

Multilevel shape optimization algorithm

Given $\mathbf{p}_1^{(1),\text{init}}, \ldots, \mathbf{p}_s^{(1),\text{init}}$

Discretize at the first level $\longrightarrow h^{(1)}, \boldsymbol{\mathcal{A}}^{(1)}(\mathbf{p}_1^{(1),\text{init}}, \ldots, \mathbf{p}_s^{(1),\text{init}})$

Solve by a quasi-Newton method coupled with the nested Newton method, while using a nested direct solver: $\mathbf{p}_1^{(1),\text{init}}, \ldots, \mathbf{p}_s^{(1),\text{init}} \longrightarrow \mathbf{p}_1^{(1),\text{opt}}, \ldots, \mathbf{p}_s^{(1),\text{opt}}$

Store the first level preconditioner $\boldsymbol{\mathcal{C}}^{(1)} := \left[\boldsymbol{\mathcal{A}}^{(1)}(\mathbf{p}_1^{(1),\text{opt}}, \ldots, \mathbf{p}_s^{(1),\text{opt}})\right]^{-1}$

for $l = 2, \ldots$ **do**

Refine: $h^{(l-1)} \longrightarrow h^{(l)}$

Prolong: $\mathbf{p}_1^{(l-1),\text{opt}}, \ldots, \mathbf{p}_s^{(l-1),\text{opt}} \longrightarrow \mathbf{p}_1^{(l),\text{init}}, \ldots, \mathbf{p}_s^{(l),\text{init}}$

Solve by a quasi-Newton method coupled with the nested Newton method, while using the nested conjugate gradients method preconditioned with $\mathbf{C}^{(l-1)}$: $\mathbf{p}_1^{(l),\text{init}}, \ldots, \mathbf{p}_s^{(l),\text{init}} \longrightarrow \mathbf{p}_1^{(l),\text{opt}}, \ldots, \mathbf{p}_s^{(l),\text{opt}}$

Store the l–th level multigrid preconditioner $\boldsymbol{\mathcal{C}}^{(l)} \approx \left[\boldsymbol{\mathcal{A}}^{(l)}(\mathbf{p}_1^{(l)}, \ldots, \mathbf{p}_s^{(l)})\right]^{-1}$

end for

5 Numerical Results

We consider a problem depicted in Fig. 2 **(a)**, which is a simplification of the direct electric current (DC) electromagnet depicted in Fig. 3 **(b)**. Some results on the usage and mathematical modeling of such electromagnets can be found in [Pos02, Luk04], respectively. Our aim is to find a distribution of the ferromagnetic material so that the generated magnetic field is strong and homogeneous enough. Unfortunately, these assumptions are contradictory and we have to balance them. The cost functional reads as follows:

$$J(u) := \int_{\Omega_\text{m}} \|\mathbf{curl}(u) - B_\text{m}^\text{avg}(u)\,(0,1)\|^2 \, d\mathbf{x} + p_B \left(\min\{0, B_\text{m}^\text{avg}(u) - B^\text{min}\}\right)^2,$$

where $\Omega_\text{m} \subset \Omega$ is the subdomain where the magnetic field should be homogeneous, $\mathbf{curl}(u) := (\partial u/\partial x_2, -\partial u/\partial x_1)$, $B_\text{m}^\text{avg}(u)$ is the mean value of the magnetic field component $-\partial u/\partial x_1$ over Ω_m, $B^\text{min} := 0.12\,[\text{T}]$ is the required minimal field and $p_B := 10^6$ is the penalty of the minimal field constraint. There are 600 turns pumped by the current of $5\,[\text{A}]$, which is averaged into a current density J being constant in the coil subdomain and vanishing elsewhere. The nonlinear material reluctivity function is $\nu(\eta) = (\nu_0 - \nu_1)\left(\frac{\eta^4}{\eta^4 + \nu_0^{-1}} - 1\right)$, where $\nu_1 := \nu_0/5100$ is the linearized reluctivity of the used ferromagnetics.

The coarsely optimized topology of the quarter of the geometry is depicted in Fig. 2 **(b)**. We chose $p_\rho := 100$ and the very initial guess was $\rho := 0.5$ in Ω_d. In the coarse topology optimization problem there were 861 design, 1105 state variables and the optimization was done in 7 steepest descent iterations, which took 2.5 seconds. Further, we approximated the boundary of the black

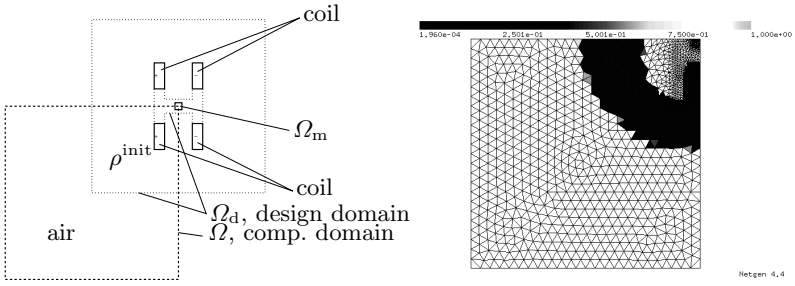

Fig. 2. Topology optimization: **(a)** initial design; **(b)** coarsely optimized design ρ^{opt}

domain by three Bézier curves described by 19 parameters in total. Solving the corresponding least square problem was finished in 8 quasi-Newton iterations, which took 26 seconds when using a forward numerical differentiation scheme. At the end, we proceeded with the multilevel shape optimization starting from the optimized curves of the previous fitting problem. The performance of this last step can be seen from Table 1. Note that from the sixth column of the table, we can see that the linear system $\mathbf{A}$ was solved almost in the optimal way (6 PCG iterations at worst), however, solution to the linearized system $\mathbf{A}'_{\mathbf{u}}$ deteoriates. This is due to the fact that we only used the preconditioner for the linear part, which did not bring any extra cost within one PCG iteration.

Table 1. Multilevel shape optimization

level	design variables	outer iters.	state variables	max. inner iters.	PCG steps lin./nonlin.	time
1	19	10	1098	3	direct	32s
2	40	15	4240	3	3/14–25	2min 52s
3	82	9	16659	4	4–5/9–48	9min 3s
4	166	10	66037	4	4–6/13–88	49min 29s
5	334	13	262953	5	3–6/20–80	6h 36min

The final result is depicted in Fig. 3 **(a)** and it is very similar to the existing geometry of the so-called O-Ring electromagnet, see Fig. 3 **(b)**.

6 Conclusion

This paper presented a method which sequentially combines topology and shape optimization. First, we solved a coarsely discretized topology optimization problem. Then, we approximated some chosen interfaces by Bézier shapes.

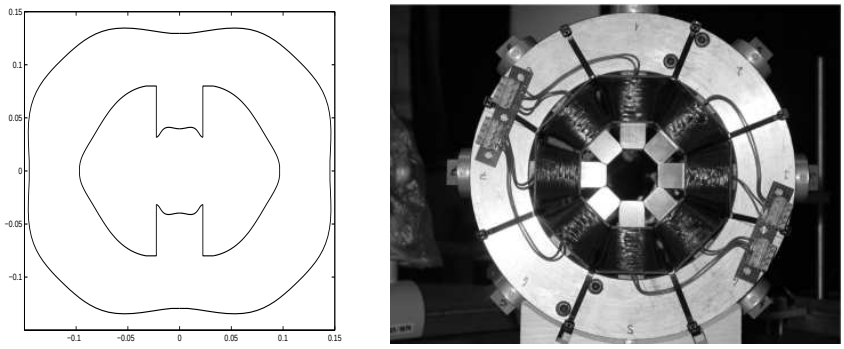

Fig. 3. Multilevel shape optimization: **(a)** optimized geometry; **(b)** the O-Ring electromagnet

Finally, we proceeded with shape optimization in a multilevel way. We applied the method to a 2-dimensional optimal shape design of a DC electromagnet, for which we achieved fine optimized geometries in terms of minutes. It remains to analyze and improve the multigrid convergence, particularly, in case of the nonlinear state operator.

References

[Ben95] Bendsøe, M.P.: Optimization of Structural Topology, Shape and Material. Springer, Berlin, Heidelberg (1995)

[Cea00] Céa, J., Garreau, S., Guillaume, P., Masmoudi, M.: The shape and topological optimizations connection. Comput. Methods Appl. Mech. Eng. **188**, 713–726 (2000)

[GW92] Gonzalez R.C., Woods R.E.: Digital Image Processing, Addison Wesley (1992).

[HN97] Haslinger J., Neittaanmäki P.: Finite Element Approximation for Optimal Shape, Material and Topology Design. Wiley, Chinchester (1997)

[Luk04] Lukáš, D.: On solution to an optimal shape design problem in 3-dimensional magnetostatics. Appl. Math. **49**:5, 24 pp. (2004)

[OBR91] Olhoff, N., Bendsøe, M.P., Rasmussen, J.: On CAD-integrated structural topology and design optimization. Comp. Meth. Appl. Mech. Eng. **89**, 259–279 (1991)

[Pos02] Postava, K., Hrabovský, D., Pištora, J., Fert, A.R., Višňovský, Š., Yamaguchi, T.: Anisotropy of quadratic magneto-optic effects in reflection. J. Appl. Phys. **91**, 7293–7295 (2002)

[TCh01] Tang, P.-S., Chang, K.-H.: Integration of topology and shape optimization for design of structural components. Struct. Multidisc. Optim. **22**, 65–82 (2001)